Effect of Calcitonin on Bone Formation and Resorption: Mathematical Modeling Approach

Chontita Rattanakul and Sahattaya Rattanamongkonkul

***Abstract*—**We study the effect of calcitonin on bone formation and resorption mathematically by developing a system of nonlinear differential equations to describe the process. The model accounts for the concentration of calcitonin above the basal level, the number of active osteoclastic cells and the number of the active osteoblastic cells. We then applied the singular perturbation to our model in order to obtain the conditions on the system parameters for which the various kinds of dynamic behavior can be occurred. Computer simulations are also carried out to support our theoretical predictions. The results show that a periodic behavior can be expected corresponding to the pulsatile secretion pattern of calcitonin observed clinically in normal individuals.

***Keywords*—**bone formation, bone resorption, calcitonin, mathematical model, singular perturbation.

I. Introduction

In adult human body, about 99% of total body calcium is stored in bone. Apart from providing structural support, bone serves as an enormous reservoir for calcium salts. About 600 mg of calcium is exchanged between bone and the extracellular fluid per day mostly through the bone resorption and formation process [1]. There are two types of cells that responsible for bone formation and resorption process which are osteoclasts, bone resorbing cells, and osteoblasts, bone forming cells. Bone remodeling process can be described step by step as follows. At first, osteoclasts appear on a previously inactive surface of bone and then, they excavate a lacuna on the surface of cancellous bone or resorption tunnel in cortical bone. After that, osteoclasts are then subsequently replaced by osteoblasts and finally, osteoblasts refill the resorption cavity and becoming osteocytes, the inactive form of osteoblasts [2], [3]. If osteoclasts produce an excessively deep resorption space, if the osteoblasts fail to completely refill the resorption space, or if both events occur then bone imbalance exists and that leads to osteoporosis [2], [3].

Manuscript received August 3, 2011. This work was supported by the Centre of Excellence in Mathematics, Commission on Higher Education, Thailand and the Faculty of Science, Mahidol University, Thailand.

C. Rattanakul is with the Department of Mathematics, Faculty of Sciences, Mahidol University, Thailand and the Centre of Excellence in Mathematics, the Commission on Higher Education, Thailand (corresponding author, phone: 662-201-5340; fax: 662-201-5343; e-mail: sccrt@mahidol.ac.th).

S. Rattanamongkonkul is with the Department of Mathematics, Faculty of Sciences, Burapha University, Thailand and the Centre of Excellence in Mathematics, the Commission on Higher Education, Thailand (e-mail: sahattay@buu.ac.th).

Osteoporosis is a major health disorder of bone remodeling occurring frequently in women especially in postmenopausal women [4]. It is characterized by low bone mass resulting from the net increase of bone resorption over bone deposition and hence bones become brittle and fracture easily [4], [5]. Many factors involve in bone remodeling process including calcitonin (CT), parathyroid hormone (PTH), vitamin D, prolactin and estrogen. Therefore, a thorough understanding of the bone remodeling process as well as the involving hormonal action are needed.

Even though there are many mathematical models proposed to describe bone remodeling process [6]-[9], none of them concentrate on the effect of calcitonin. Therefore, in this paper, we will develop a system of nonlinear differential equations to describe bone remodeling process based on the effect of calcitonin.

II. Model Development

Let us denote the concentration of CT above the basal level in blood at time t by $X(t)$, the number of active osteoclasts at time t by $Y(t)$, and the number of active osteoblasts at time t by $Z(t)$. We also assume that the high levels of osteoclast and osteoblast precursors lead to the high levels of active osteoclastic and osteoblastic cells, respectively, which result from the differentiation, and activation of their precursors.

Firstly, CT is produced by the thyroid gland [1]. The elevated serum calcium level stimulates the secretion of CT. In order to counter balance the high level of calcium, CT inhibits bone resorption by inhibiting osteoclastic activity resulting in decreasing serum calcium [1]. Therefore, the equation for the rate of calcitonin secretion is then assumed to have the form

$$\frac{dX}{dt} = \left(\frac{a_1 + a_2 Y}{k_1 + Y} \right) - b_1 X \tag{1}$$

where the first term on the right-hand side of (1) represents the secretion rate of CT from parafollicular cells in the thyroid gland. The last term is the removal rate constant b_1. a_1, a_2 and k_1 are positive constants.

Secondly, osteoclasts are responsible for bone resorption. They are large cells that arise by fusion of mononucleated hematopoietic cells [1]. Differentiation and activation of osteoclasts require direct physical contact with osteoblastic cells that govern these processes by producing at least two

cytokines [1]. Many factors involve in the regulation of osteoclast formation and differentiation such as osteoclast differentiation factor (ODF) which was found to be identical to osteoprotegerin ligand (OPGL), TNF-related activation induces cytokine (TRANCE), receptor activator NF-kB ligand (RANKL) [6],[10],[11]. Therefore, the dynamics of the active osteoclastic population can be described by the following equation

$$\frac{dY}{dt}=\left(a_3-\frac{a_4X}{k_2+X^2}\right)YZ-b_2Y \tag{2}$$

where the first term on the right-hand side of (2) represents the reproduction of active osteoclasts and the inhibitory effect of calcitonin on active osteoclasts reproduction. The last term represents the removal rate of active osteoclasts from the system. a_3, a_4, b_2 and k_2 are positive constants.

Finally, osteoblasts are responsible for bone formation. They arise from progenitors in connective tissue and marrow stroma and form a continuous sheet on the surface of newly forming bone [1]. There are many factors involve in the proliferation and differentiation of osteoblasts such as FGF, IGF-I, TGF-beta. On the other hand, CT has also been found to enhance osteoblastic bone formation [12], [13]. The dynamics of the osteoblastic population can be described by the following equation

$$\frac{dZ}{dt}=\left(\frac{a_5+a_6X}{k_3+X}\right)Z-b_3Z \tag{3}$$

where the first term on the right-hand side of (3) represents the stimulating effect of CT on the reproduction of active osteoblasts. The last term is the removal rate of active osteoblasts from the system. a_5, a_6, b_3 and k_3 are positive constants.

III. SINGULAR PERTURBATION ANALYSIS

To apply the singular perturbation technique to our model, we assume that the dynamics of CT is fast. The osteoclastic population possesses the intermediate dynamics and the osteoblastic population has the slow dynamics. Consequently, we scale the dynamics of the three components and parameters of the system in term of small positive parameters $0<\varepsilon<<1$ and $0<\delta<<1$ as follows.

Letting $x=X,\ y=Y,\ z=Z,\ c_1=a_1,\ c_2=a_2,\ c_3=\frac{a_3}{\varepsilon},$ $c_4=\frac{a_4}{\varepsilon}, c_5=\frac{a_5}{\varepsilon\delta}, c_6=\frac{a_6}{\varepsilon\delta}, d_1=b_1, d_2=\frac{b_2}{\varepsilon}, d_3=\frac{b_3}{\varepsilon\delta},$ we are led to the following model equations:

$$\frac{dx}{dt}=\left(\frac{c_1+c_2y}{k_1+y}\right)-d_1x\equiv f(x,y,z) \tag{4}$$

$$\frac{dy}{dt}=\varepsilon\left(\left(c_3-\frac{c_4x}{k_2+x^2}\right)yz-d_2y\right)\equiv\varepsilon g(x,y,z) \tag{5}$$

$$\frac{dz}{dt}=\varepsilon\delta\left(\left(\frac{c_5+c_6x}{k_3+x}\right)z-d_3z\right)=\varepsilon\delta h(x,y,z) \tag{6}$$

The system of (4)-(6), with the small parameters ε and δ can then be analyzed by using the geometric singular perturbation method which, under suitable regularity conditions, allows approximating the solution of the system with a sequence of simple dynamic transitions occurring at different speeds.

The shapes and relative positions of the manifolds $\{f=0\}, \{g=0\}$ and $\{h=0\}$ determine the shapes, directions and speeds of the solution trajectories. We now analyze each of the equilibrium manifolds in detail.

The manifold $\{f=0\}$

This manifold is given by the equation

$$x=\frac{1}{d_1}\left(\frac{c_1+c_2y}{k_1+y}\right)\equiv U(y) \tag{7}$$

which is parallel to the z-axis. It intersects the $(x,z)-$plane along the line

$$x=\frac{c_1}{d_1k_1}\equiv x_1 \tag{8}$$

Moreover, $U(y)$ is an increasing function of x and $U(y)\to\frac{c_2}{d_1}\equiv x_2$ as $y\to\infty$.

The manifold $\{g=0\}$

This manifold consists of two submanifolds. One is the trivial manifold $y=0$. The nontrivial one given by the equation

$$z=\frac{d_2\left(k_2+x^2\right)}{c_3\left(k_2+x^2\right)-c_4x}\equiv V(x) \tag{9}$$

this nontrivial manifold is independent of the variable y and thus this submanifold is parallel to the y-axis with asymptotic line

$$z=\frac{d_2}{c_3}\equiv z_2 \tag{10}$$

Furthermore, the nontrivial manifold $\{g=0\}$ attains its maximum at the point where

$$x=\sqrt{k_2}\equiv x_3 \quad \text{and} \quad z=\frac{2d_2k_2}{2c_3k_2-c_4\sqrt{k_2}}\equiv z_1 \tag{11}$$

The manifold $\{h=0\}$

This consists of the trivial manifold $z=0$ and the nontrivial one given by the equation

$$x=\frac{d_3k_3-c_5}{c_6-d_3}\equiv x_4 \tag{12}$$

Case I: If ε and δ are sufficiently small and the inequalities

$$0 < x_1 < x_4 < x_2, \tag{13}$$

$$z_2 < z_1, \tag{14}$$

$$c_4 < 2c_3\sqrt{k_2}, \tag{15}$$

$$c_6 < d_3, \tag{16}$$

and

$$d_3 k_3 < c_5 \tag{17}$$

are satisfied where all the parametric values are given as above, then the manifolds are positioned as in Fig. 1 and the system of (4)-(6) will have a periodic solution. Here, the transitions of slow, intermediate and high speeds are indicated by one, two and three arrows, respectively.

In Fig. 1, without loss of generality we start from point *I* and we assume that the position of *I* is as in Fig. 1 with $\{f \neq 0\}$. A fast transition will tend to point *J* on the manifold $\{f = 0\}$. Here, $\{g < 0\}$ and a transition at intermediate speed will be made in the direction of decreasing y until point *K* on the curve $\{f = g = 0\}$ is reached. A slow transition then follows along this curve to some point *L* where the stability of submanifold will be lost. A jump to point *M* on the other stable part of $\{f = g = 0\}$ followed by a slow transition in the direction of decreasing z until the point *N* is reached since $\{h < 0\}$ here. Once the point *N* is reached the stability of submanifold will be lost. A jump to point *O* on the other stable part of $\{f = g = 0\}$ followed by a slow transition in the direction of increasing *z* since $\{h > 0\}$ here. Consequently, a slow transition will bring the system back to the point *L*, followed by flows along the same path repeatedly, resulting in the closed orbit *LMNOL*. Thus, limit cycle in the system for ε and δ are sufficiently small exists.

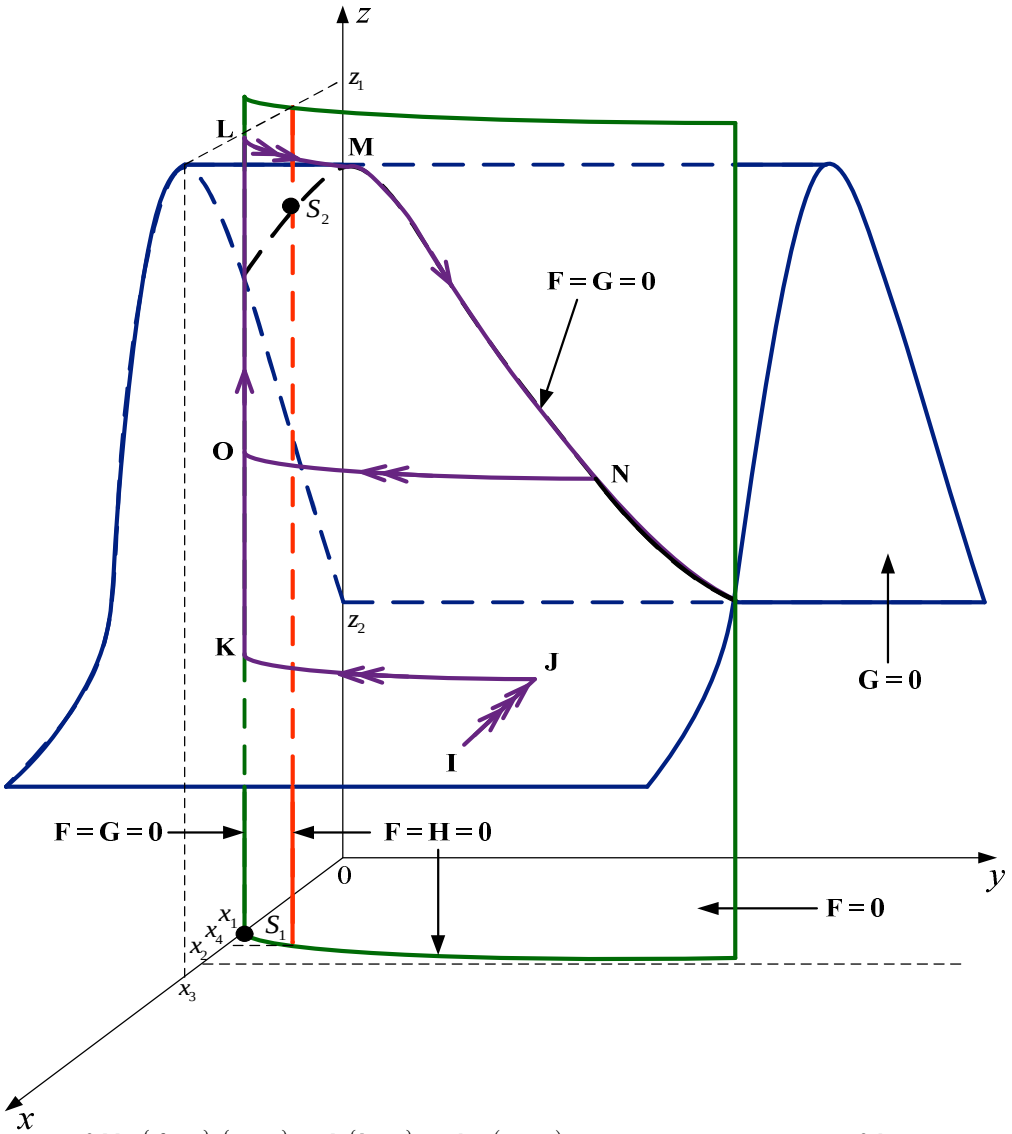

Fig. 1 The three equilibrium manifolds $\{f = 0\}, \{g = 0\}$ and $\{h = 0\}$ in the (x, y, z) – space in Case 1. Segments of the trajectories with one, two, and three arrows represent slow, intermediate, and fast transitions, respectively.

Case II: If ε and δ are sufficiently small and the inequalities

$$0 < x_3 < x_1 < x_4 < x_2, \tag{18}$$

$$z_2 < z_1, \tag{19}$$

$$c_4 < 2c_3\sqrt{k_2}, \tag{20}$$

$$c_6 > d_3, \tag{21}$$

and

$$d_3 k_3 > c_5 \tag{22}$$

are satisfied where all the parametric values are given as above, then the manifolds are positioned as in Fig. 2 and the system of (4)-(6) will have a stable equilibrium point.

In Fig. 2, without loss of generality, we start from point I and we assume that the position of I is as in Fig. 2 with $\{f \neq 0\}$. A fast transition will bring the solution trajectory to point J on the manifold $\{f = 0\}$. Here, $\{g < 0\}$ and a transition at intermediate speed will be made in the direction of decreasing y until point K on the curve $\{f = g = 0\}$ is reached followed by a slow transition in the direction of decreasing z until the steady state S_1 where $f = g = h = 0$ is reached since $\{h < 0\}$ here. Thus, the solution trajectory is expected in this case to tend toward this stable equilibrium point S_1 as time passes.

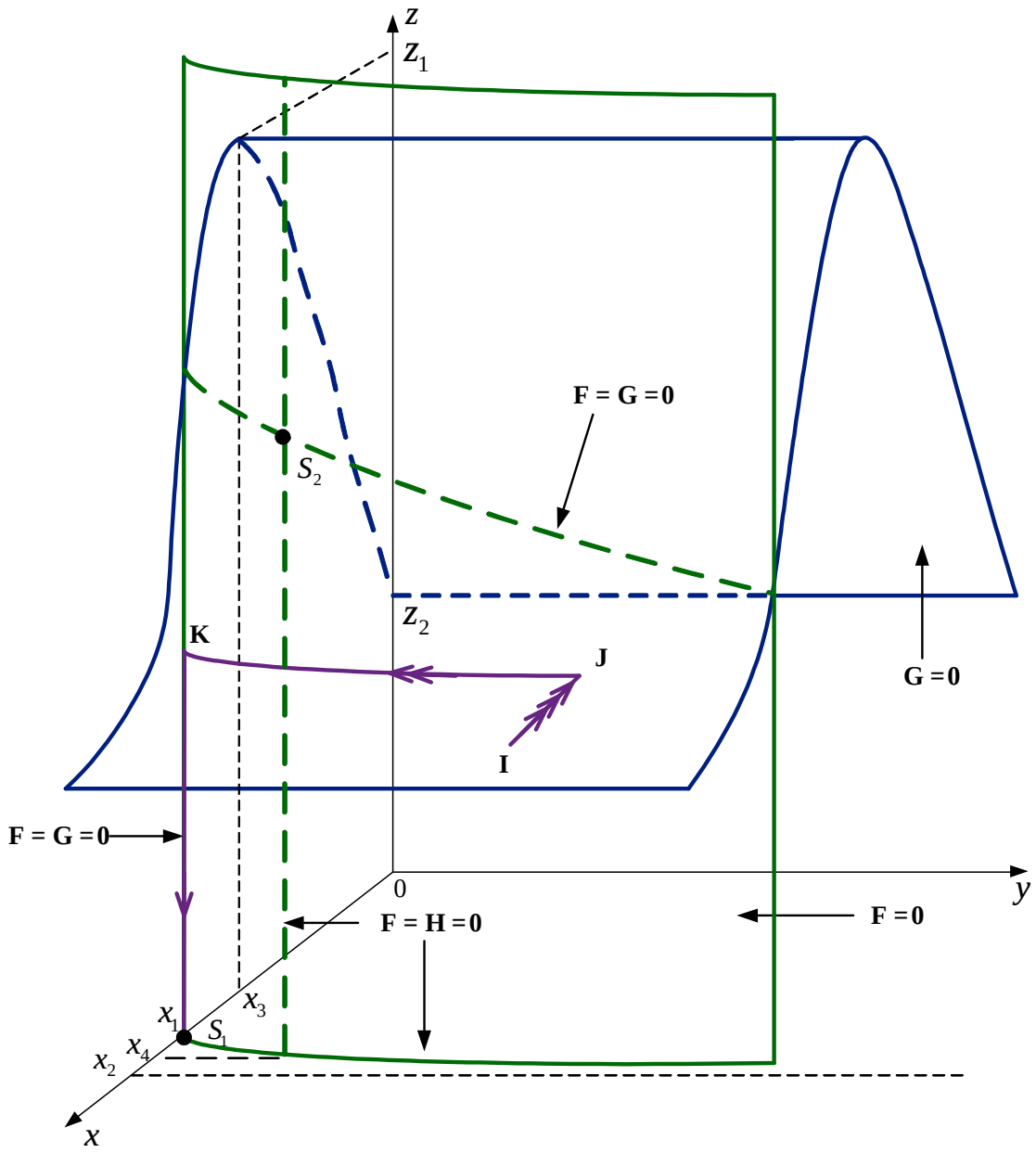

Fig. 2 The three equilibrium manifolds $\{f = 0\}, \{g = 0\}$ and $\{h = 0\}$ in the (x, y, z) – space in Case 2. Segments of the trajectories with one, two, and three arrows represent slow, intermediate, and fast transitions, respectively.

Case III: If ε and δ are sufficiently small and

$$0 < x_1 < x_4 < x_2, \tag{23}$$

$$z_2 < z_1, \tag{24}$$

$$c_4 < 2c_3\sqrt{k_2}, \tag{25}$$

$$c_6 > d_3, \tag{26}$$

and

$$d_3k_3 > c_5 \tag{27}$$

are satisfied where all the parametric values are given as above, then the manifolds are positioned as in Fig. 3 and the system of (4)-(6) will have a stable equilibrium point.

In Fig. 3, without loss of generality, we start from point I and we assume that the position of I is as in Fig. 3 with $\{f \neq 0\}$. A fast transition will bring the solution trajectory to point J on the manifold $\{f = 0\}$. Here, $\{g < 0\}$ and a transition at intermediate speed will be made in the direction of decreasing y until point K on the curve $\{f = g = 0\}$ is reached followed by a slow transition in the direction of decreasing z until the steady state S_1 where $f = g = h = 0$ is reached since $\{h < 0\}$ here. Thus, the solution trajectory is expected in this case to tend toward this stable equilibrium point S_1 as time passes.

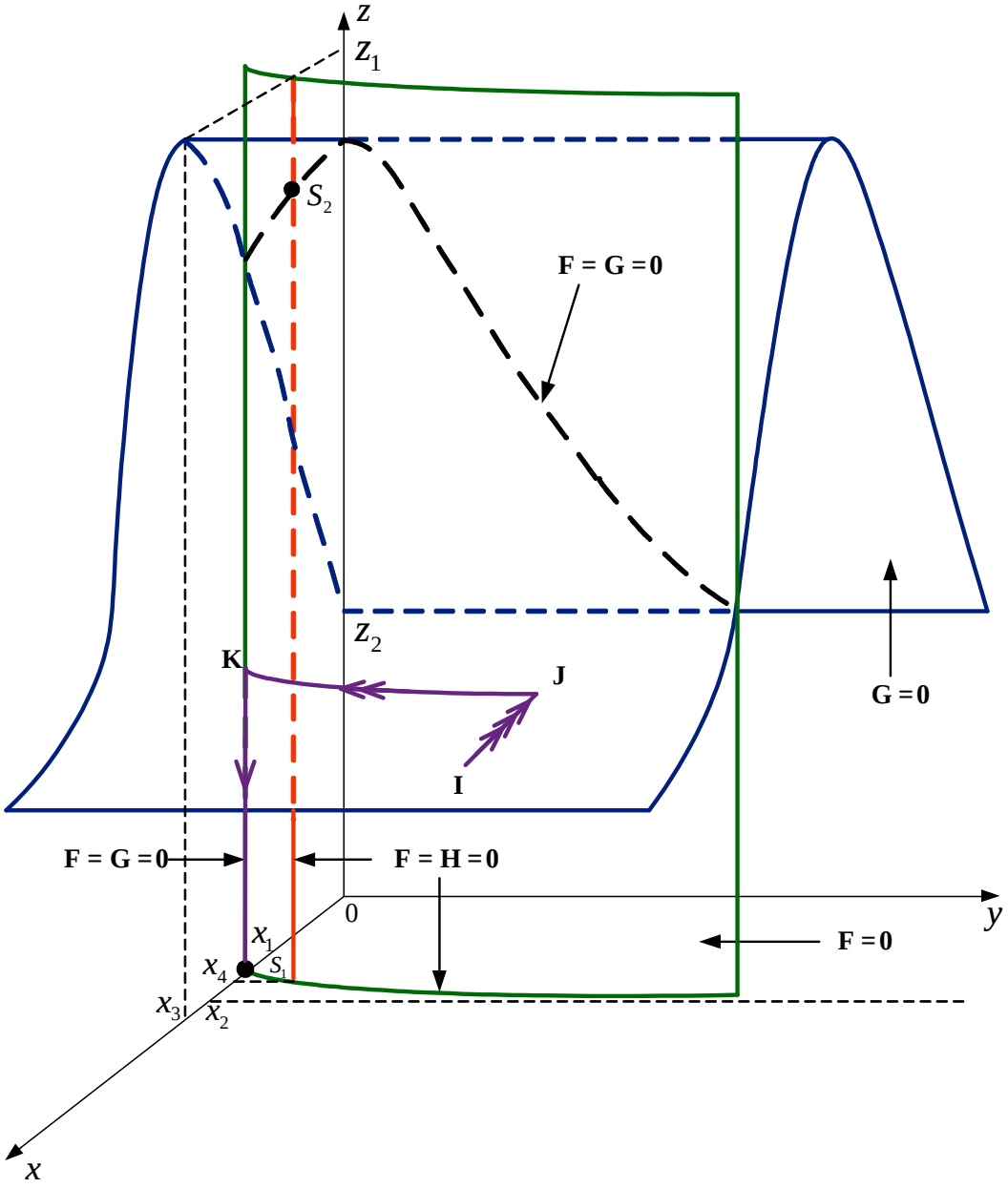

Fig. 3 The three equilibrium manifolds $\{f = 0\}, \{g = 0\}$ and $\{h = 0\}$ in the (x, y, z) – space in Case 3. Segments of the trajectories with one, two, and three arrows represent slow, intermediate, and fast transitions, respectively.

IV. COMPUTER SIMULATIONS

A numerical result of the system (4)-(6) is presented in Fig. 4, with parametric values chosen to satisfy the condition in Case 1. The solution trajectory, shown in Fig. 4a project onto the (x,z)-plane, tends to a limit cycle as theoretically predicted. The corresponding time courses of the calcitonin concentration and the number of active osteoblasts are as shown in Fig. 4b and 4c, respectively.

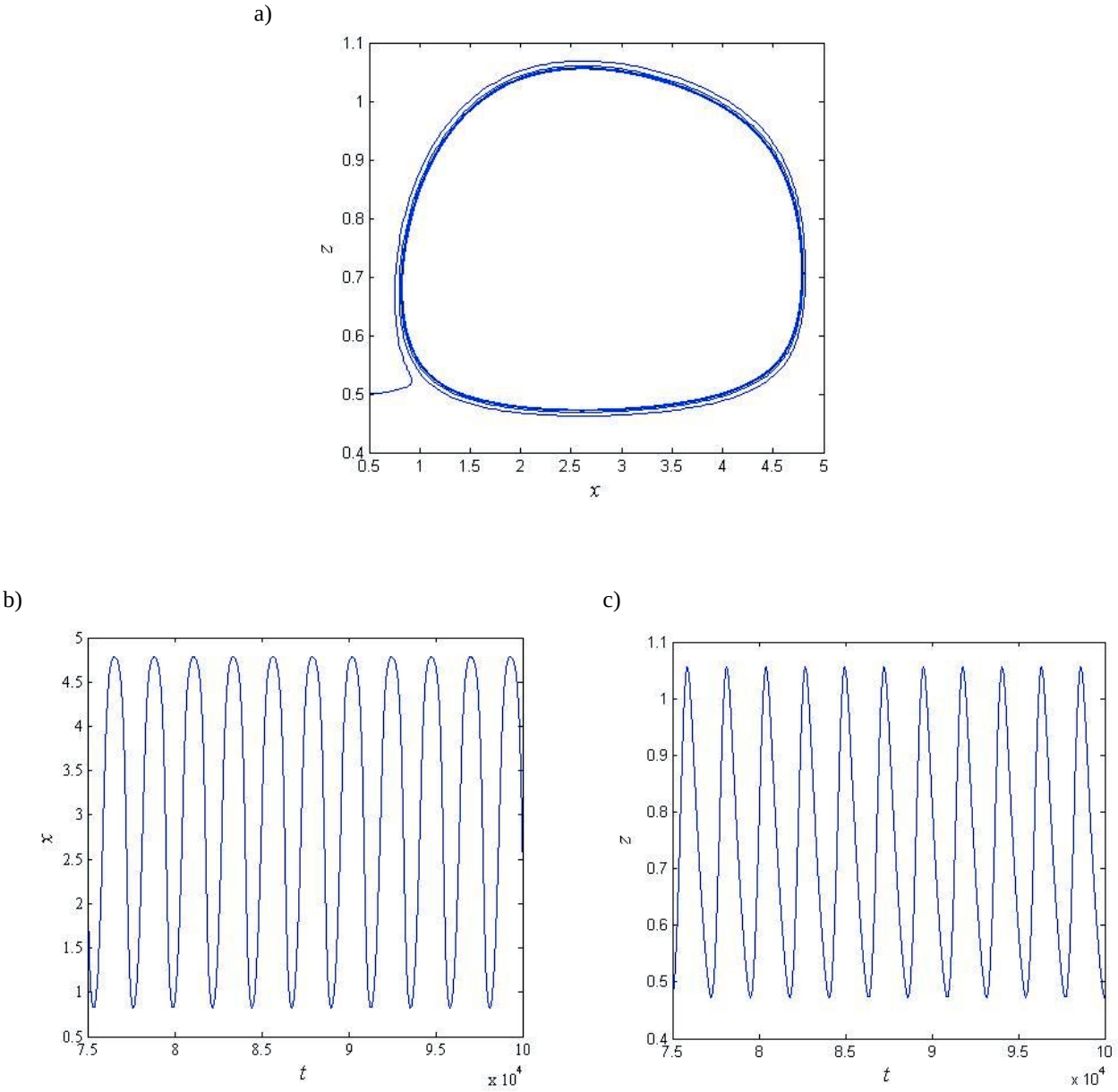

Fig. 4 A computer simulation of the model systems (4)-(6) with $c_1 = 0.1, c_2 = 0.5, c_3 = 0.4, c_4 = 0.7, c_5 = 0.7,\ c_6 = 0.085, k_1 = 3,\ k_2 = 5,\ k_3 = 2,\ d_1 = 0.1,\ d_2 = 0.2,\ d_3 = 0.2,\ \varepsilon = 0.1,\ \delta = 0.2,\ x(0) = 0.5, y(0) = 0.5,\ z(0) = 0.5.$ (a) The solution trajectory projected onto the (*x*,*z*)-plane. (b) The corresponding time courses of calcitonin concentration (*x*), and (c) number of active osteoblastic cells (*z*).

A numerical result of the system (4)-(6) is presented in Fig. 5, with parametric values chosen to satisfy the condition in Case 2. The solution trajectory, shown in Fig. 5a project onto the (x, y)-plane, tends to a stable equilibrium as theoretically predicted. The corresponding time courses of the calcitonin concentration and the number of active osteoclasts are as shown in Fig. 5b and 5c, respectively.

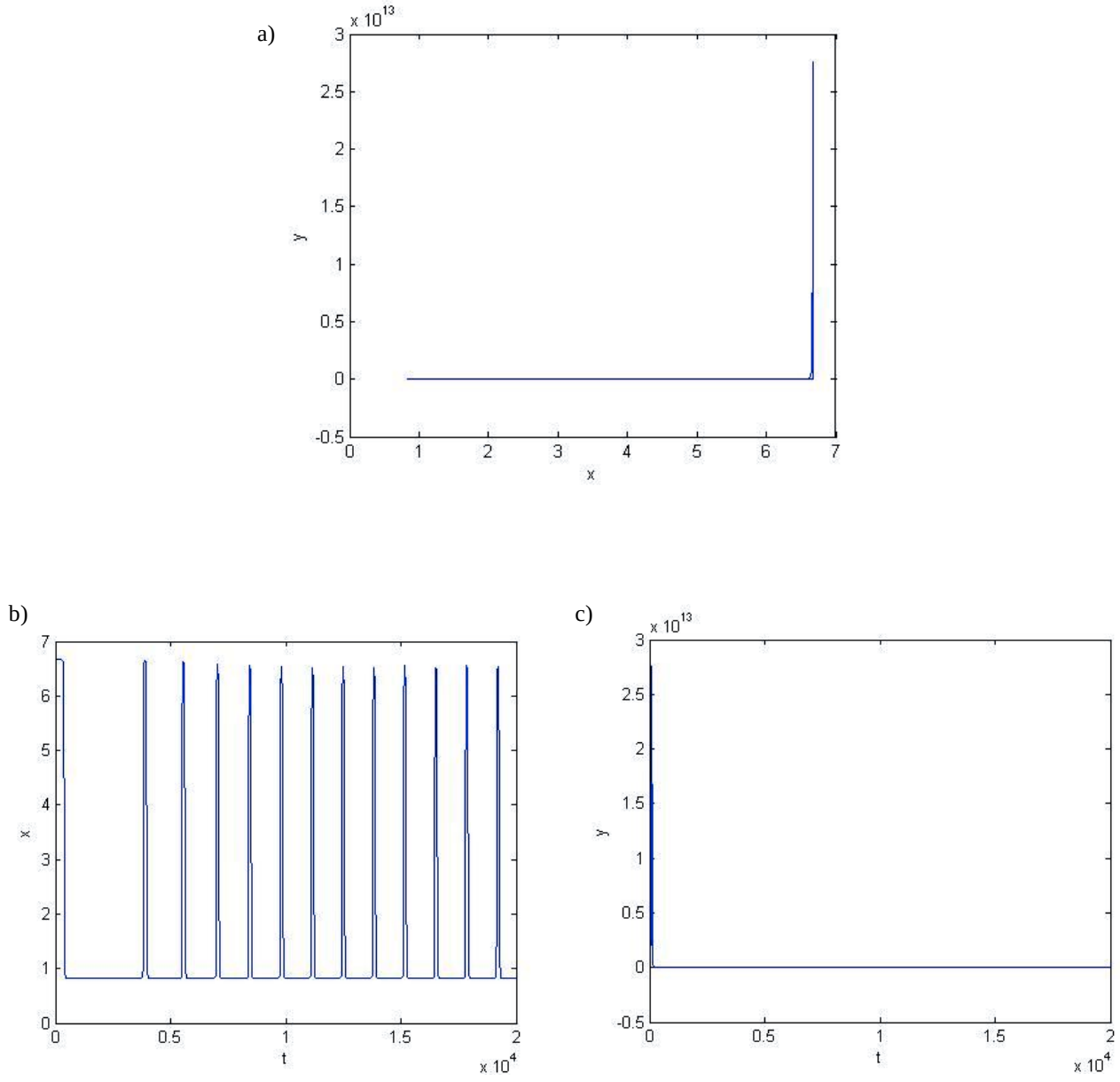

Fig. 5 A computer simulation of the model systems (4)-(6) with $c_1 = 0.5, c_2 = 0.7, c_3 = 0.2, c_4 = 0.7, c_5 = 0.1$, $c_6 = 0.21, k_1 = 3$, $k_2 = 4$, $k_3 = 1$, $d_1 = 0.05$, $d_2 = 0.2$, $d_3 = 0.2$, $\varepsilon = 0.01$, $\delta = 0.01$, $x(0) = 1$, $y(0) = 5$, $z(0) = 5$. (a) The solution trajectory projected onto the (x,y)-plane. (b) The corresponding time courses of calcitonin concentration (x), and (c) number of active osteoclastic cells (y).

A numerical result of the system (4)-(6) is presented in Fig. 6, with parametric values chosen to satisfy the condition in Case 3. The solution trajectory, shown in Fig. 6a project onto the (x, y)-plane, tends to a stable equilibrium as theoretically predicted. The corresponding time courses of the calcitonin concentration and the number of active osteoclasts are as shown in Fig. 6b and 6c, respectively.

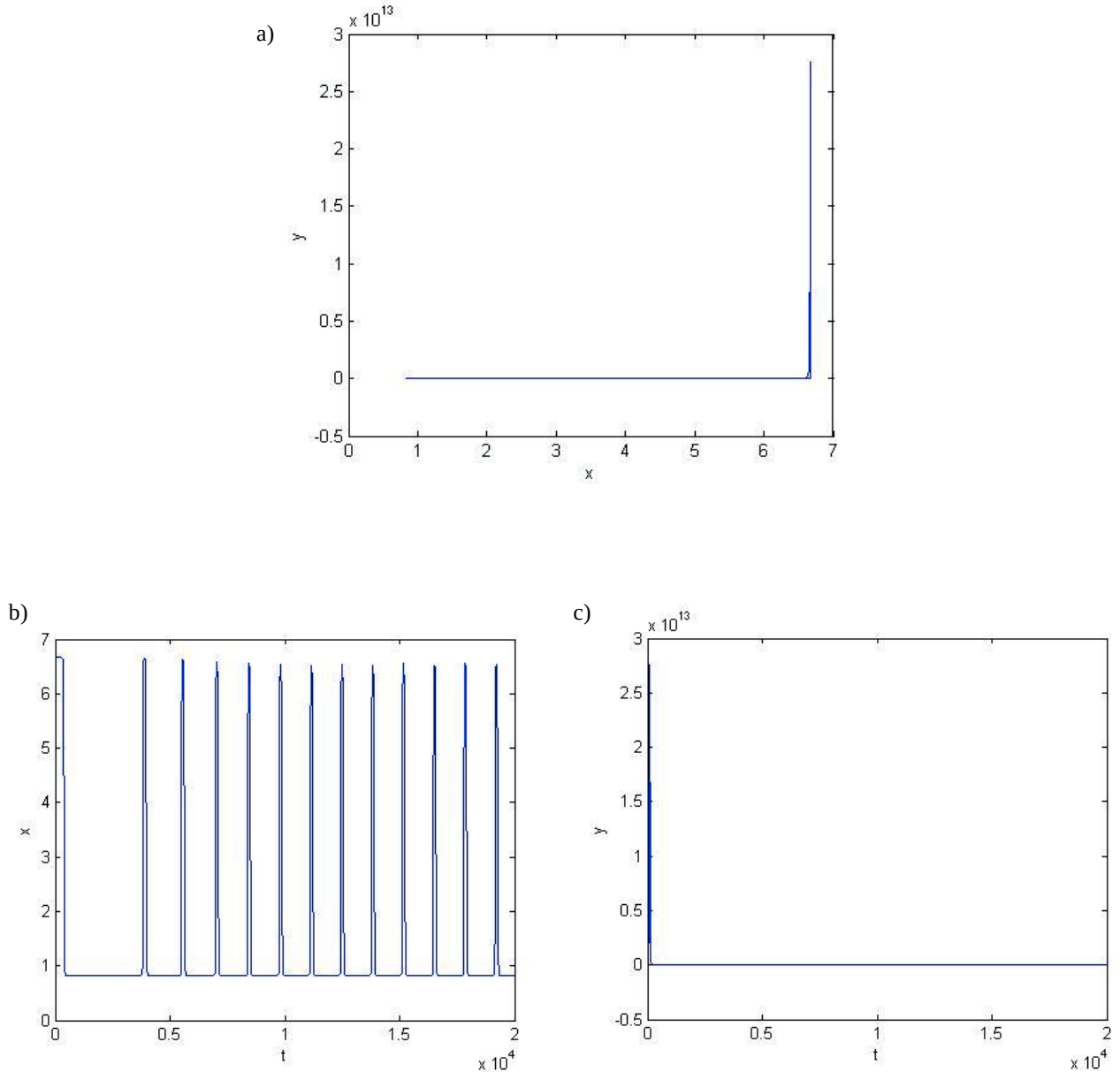

Fig. 6 A computer simulation of the model systems (4)-(6) with $c_1 = 0.6, c_2 = 0.7, c_3 = 0.2, c_4 = 0.7, c_5 = 0.1$, $c_6 = 0.21, k_1 = 3$, $k_2 = 4$, $k_3 = 1$, $d_1 = 0.05$, $d_2 = 0.2$, $d_3 = 0.2$, $\varepsilon = 0.01$, $\delta = 0.01$, $x(0) = 1$, $y(0) = 5$, $z(0) = 5$. (a) The solution trajectory projected onto the (x,y)-plane. (b) The corresponding time courses of calcitonin concentration (x), and (c) number of active osteoclastic cells (y).

V. CONCLUSION

In this paper, bone formation and resorption is studied mathematically. We have proposed a system of nonlinear differential equations accounting for the level of calcitonin, the number of active osteoclasts, and the number of active osteoblasts as in (1)-(3). The singular perturbation technique [14], [15] is then applied to analyzed our model to obtain the conditions on the system parameters for which the various kinds of dynamics behavior can be occurred including a periodic behavior in the solution of the system. Computer simulations of the model are then carried out by using Runge-Kutta method which has been widely used to find the approximate solution of the differential equations [16]-[19]. Both of theoretical and numerical results show that the periodic behavior can be exhibited by our model which closely resembles to the serum level of calcitonin that has been observed clinically [20], even though the model is kept relatively simple.

REFERENCES

[1] H.M. Goodman, *Basic Medical Endocrinology*, 3rd edition, Academic Press, 2003.

[2] T. Russell, B. Turner, R. Lawrence, C.S. Thomas," Skeletal effects of estrogen", *Endocr. Rev.*, vol. 15, no. 3, pp.275-300, 1994.

[3] L.G. Raisz and B. E. Kream," Regulation of bone formation", *New Engl. J. Med.*, vol. 309, pp.29-35, 1983.

[4] R.A. Lobo, J.L. Kelsey and R. Marcus, *Menopause: Biology and Pathobiology*, Academic Press, 2000, pp. 287-307.

[5] A. Rosenberg, *Skeletal system and soft tissue tumors, in Robbins Pathologic Basis of Disease*, 5th edition, R. S. Cotran, V. Kumar and S. L. Robbins (Eds), Philadelphia: W. B. Saunders Co., 1994, pp.1219-1222.

[6] M.H. Kroll, "Parathyroid hormone temporal effects on bone formation and resorption", *Bull. Math. Bio*, vol. 62, pp.163-188, 2000.

[7] C. Rattanakul, Y. Lenbury, N. Krishnamara and D.J. Wollkind, "Mathematical modelling of bone formation and resorption mediated by parathyroid hormone: Responses to estrogen/PTH therapy", BioSystems, vol. 70, pp. 55-72, 2003.

[8] P. Pivonka, J. Zimak, D.W. Smith, B.S. Gardiner, C.R. Dunstan, N.A. Sims, T.J. Martin, G.R. Mundy, "Model structure and control of bone remodeling: A theoretical study", *Bone*, 43, 249-263, 2008.

[9] S.V. Komarova, "Mathematical model of paracrine interactions between osteoclasts and osteoblasts predicts anabolic action of parathyroid hormone on bone", *Endocrinology*, 146(8), pp. 3589-3595, 2005.

[10] H. Yasuda, N. Shima and N. Nakagawa, "Osteoclast differentiation factor is a ligand for osteoprotogerin/osteoclast inhibitory factor and identical to TRANCE/RANKL", *Proc Natl Acad Sci USA*, vol. 95, no. 7, pp. 3597-3602, 1998.

[11] S.K. Lee and J.A. Lorenzo, "Parathyroid hormone stimulates TRANCE and inhibits osteoprotegerin massenger ribonucleic acid expression in murine bone marrow cultures: correlation with osteoclast-like cell formation", *Endocrinology*, vol. 140, no. 8, pp. 3552-3561, 1999.

[12] S. Wallach, J.R. Farley, D.J. Baylink and L.B. Gati, "Effects of calcitonin on bone quality and osteoblastic function", *Calcif. Tissue Int.*, vol. 52, no. 5, pp. 335-339, 1993.

[13] Q.X. Tian, G.Y. Huang, J.L. Zhou, Q.H. Liu and X.R. Du, "Effects of calcitonin on osteoblast cell proliferation and OPG/RANKL expression: Experiment with mouse osteoblasts", *Zhonghua Yi Xue Za Zhi.*, vol. 87, no. 21, pp. 1501-1505, 2007.

[14] T.J. Kaper, "An introduction to geometric methods and dynamical systems theory for singular perturbation problems. Analyzing multiscale phenomena using singular perturbation methods", *Proc. Symposia Appl Math*, vol. 56, 1999.

[15] S. Rinaldi and S. Muratori, "A separation condition for the existence of limit cycle in slow-fast systems", Appl Math Modelling, vol. 15, pp. 312-318, 1991.

[16] W. Sanprasert, U. Chundang and M. Podisuk, "Integration method and Runge-Kutta method", in *Proc. 15th American Conf. on Applied Mathematics*, WSEAS Press, Houston, USA, 2009, pp. 232.

[17] M. Racila and J.M. Crolet, "Sinupros: Mathematical model of human cortical bone", in *Proc. 10th WSEAS Inter. Conf. on Mathematics and Computers in Biology and Chemistry*, WSEAS Press, Prague, Czech Republic, 2009, pp. 53.

[18] N. Razali, R. R. Ahmed, M. Darus and A.S. Rambely, "Fifth-order mean Runge-Kutta methods applied to the Lorenz system", in *Proc. 13th WSEAS Inter. Conf. on Applied Mathematics*, WSEAS Press, Puerto De La Cruz, Tenerife, Spain, 2008, pp. 333.

[19] A. Chirita, R. H. Ene, R.B. Nicolescu and R.I. Carstea, "A numerical simulation of distributed-parameter systems", in *Proc. 9th WSEAS Inter. Conf. on Mathematic*al Methods and Computational Techniques in Electrical Engineering, WSEAS Press, Arcachon, 2007, pp. 70.

[20] K. N. Muse, S. C. Manolagas, L.J. Deftos, N. Alexander, and S.S.C. Yen, "Calcium-regulating hormones across the menstrual cycle", *J. Clin. Endocrinol. Metab.*, vol.62, no.2, pp.1313-1315, 1986.